



Cite this: *Phys. Chem. Chem. Phys.*,
2024, 26, 14766

An eminent approach towards next generation solvents for sustainable packaging and stability of enzymes: a comprehensive study of ionic liquid and deep eutectic solvent mixtures†

Urooj Fatima,^a Nirmala Deenadayalu^b and Pannuru Venkatesu *^a

Hybrid ionic fluids (HIFs) are newly emerging and fascinating sustainable solvent media, which are attracting a great deal of scientific interest in protecting the native structure of proteins. For a few decades, there has been a demand to consider ionic liquids (ILs) and deep eutectic solvents (DESs) as biocompatible solvent media for enzymes; however, in some cases, these solvent media also show limitations. Therefore, this work focuses on synthesising novel HIFs to intensify the properties of existing ILs and DESs by mixing them. Herein, HIFs have been synthesised by the amalgamation of a deep eutectic solvent (DES) and an ionic liquid (IL) with a common cation or anion. Later on, the stability and activity of hen's egg white lysozyme (Lyz) in the presence of biocompatible solvent media and HIFs were studied by various techniques such as UV-vis, steady-state fluorescence, circular dichroism (CD), Fourier transform infrared spectroscopy (FT-IR) and dynamic light scattering (DLS) measurements. This work emphasises the effect of a DES (synthesised using 1:2 choline chloride and malonic acid) [Maline], ILs (1-butyl-3-methylimidazolium chloride [BMIM]Cl or choline acetate [Chn][Ac]) and their corresponding HIFs on the structure and functionality of Lyz. Moreover, we also studied the secondary structure, thermal stability, enzymatic activity and thermodynamic profile of Lyz at pH = 7 in the presence of varying concentrations (0.1 to 0.5 M) of [BMIM]Cl and [Chn][Ac] ILs, Maline as a DES, and Maline [BMIM]Cl (HIF₁) and Maline [Chn][Ac] (HIF₂). Spectroscopic results elucidate that ILs affect the activity and structural stability of Lyz. In contrast, the stability and activity are inhibited by DES and are enhanced by HIFs at all the studied concentrations. Overall, the experimental results studied explicitly elucidate that the structure and stability of Lyz are maintained in the presence of HIF₁ while these properties are intensified in HIF₂. This study shows various applications in biocompatible green solvents, particularly in the stability and functionality of proteins, due to their unique combination where the properties counteract the negative effect of either DESs or ILs in HIFs.

Received 2nd March 2024,
Accepted 20th April 2024

DOI: 10.1039/d4cp00931b

rsc.li/pccp

1. Introduction

Enzymes are often responsible for catalyzing a chemical reaction; these are specific for their substrate and show remarkable catalytic power.¹ They are found in cells and are vital in various biological functions.² The misfolding of such an enzyme has a deleterious effect which causes inactivation of the enzyme and achieves an aggregated state, which also leads to the formation of

amyloids, which are insoluble protein fibrils.³ Consequently, the mechanism of protein folding should be keenly observed. Protein folding is driven and strengthened *via* the formation of various bonds, which include hydrogen bonding, di-sulfide bonding, and ionic and hydrophobic attractions in localized conditions, and these bonds are affected by the properties of the solvent, which include temperature, pH, ionic strength and polarity.¹ Therefore, to preserve the native state of the protein, numerous approaches are involved. The most classic and contemporary approach for their stabilization is their interaction with additives.

Additives have the property of enhancing the rate of correct protein folding.^{4,5} Herein, a co-solvent, a kind of additive, is also responsible for preserving the native state of the protein *in vitro*. Among them, ionic liquids (ILs), commonly considered to be green solvents, have drawn considerable attention for stabilizing the native structure of proteins,^{4,5} since the properties of these

^a Department of Chemistry, University of Delhi, Delhi-110 007, India.
E-mail: uroojfatima816@gmail.com, venkatesup@hotmail.com,
pvenkatesu@chemistry.du.ac.in

^b Department of Chemistry, Durban University of Technology, Durban - 4000, South Africa. E-mail: nirmalad@dut.ac.za

† Electronic supplementary information (ESI) available: the supporting information (ESI) instrumentation and methods, 7 figures and 4 tables in 13 pages. See DOI: <https://doi.org/10.1039/d4cp00931b>

novel green solvents can be tailored by tuning either their cation or anion to obtain the desired changes. ILs induce protein refolding from an unfolded protein^{6–14} and act as protein stabilizing co-solvents. They have also proven themselves to be potential biocompatible solvents for the long-term stability of a protein, enhancing refolding and preventing aggregation.⁷ Apart from this, Byrne *et al.*¹⁵ reported the refolding of thermally unfolded lysozyme (Lyz) in the presence of ILs, and Mangialardo *et al.*⁵ again reported the refolding of Lyz in the presence of an ionic liquid (IL) through spectroscopic studies.

Similarly, deep eutectic solvents (DESs), considered analogues of ILs, have been reported for stabilizing, enhancing refolding, and preventing protein aggregation.¹⁶ Along with all the distinctive and unique properties of ILs, they also show low toxicity, volatility, and biodegradability. Again, the desired property can be tuned by tuning the hydrogen bond acceptor (HBA), hydrogen bond donor (HBD), or their mixing in appropriate ratios. DESs show a lot of potential applications in the field of bioinformatics. Little literature is available in which a DES has proven itself as a potential candidate for enhancing the activity and stability of proteins^{17–20} Likewise, Esquembre *et al.*²¹ reported the thermal unfolding and refolding of Lyz in DESs and their aqueous dilutions *via* intrinsic fluorescence and CD spectroscopy. Despite the enormous advantages discussed above, these two novel green solvents also have some limitations.²² For instance, barriers to the widespread adoption of ILs are that some are solid at room temperature, some possess high viscosity and require complex preparation methods, some are also toxic (an inappropriate combination of ions) and some are non-biodegradable.^{22–25} DESs also show limitations as their data on behavior and properties are limited. However, an alternative green solvent medium must be developed to address such pivotal issues that limit their applicability.

Therefore, this work intends to synthesize novel hybrid solvents, commonly termed hybrid ionic fluids (HIFs), a greener alternative to conventional volatile solvents. HIFs are prepared by mixing an equimolar ratio of an IL and a DES, which have either a common cation or a common anion. The process of amalgamation of two solvents was based on the concept of a double salt ionic liquid (DSIL).^{26,27} Very little literature is available on the applications of HIFs; likewise, Huang *et al.*²⁸ and Lian *et al.*²⁹ reported an ionic liquid formulated as a hybrid solvent for CO₂ capture. Nevertheless, Maka *et al.*³⁰ communicated the application of a mixture of a molecular IL 1-butyl-3-methyl imidazolium thiocyanate and a choline-chloride-based DES for an epoxy resin curing agent. Furthermore, Banjara *et al.*³¹ investigated the micellization behavior in the presence of an IL–DES mixture. On the other hand, a combined IL–DES was also employed for the extraction and separation of platinum, palladium and rhodium reported by Lanaridi *et al.*³² Very recently, Wang *et al.* used a novel mixture of DES/IL/water for selective extraction and separation of natural products from *Rosamarinus officinalis* leaves.³³ In addition, HIFs have proven themselves to be a greener substitute in biological applications, including enzymatic efficiency, stability, and activity. Nakka *et al.*³⁴ explained the enhancement of the properties of an HIF in the presence of stem

bromelain. The biotechnological process plays a pivotal role in imparting stability and activity to biological elements; however, based on the protein, they suffer from low stability, require low temperatures, and use excipients for storage and transformation. Thus, there is an urgent need to study novel solvents and excipients employed to stabilize proteins.

As far as we know, the HIFs synthesized here are novel and have not yet been reported for protein stabilization. To gain insight into a comparative study of choline chloride–malonic acid-based DESs, choline and imidazolium-based ILs and their HIFs were employed to explore the stability of hen's egg white protein. To assess the structural stability of Lyz in various concentrations of novel biocompatible solvents, different biophysical techniques were employed, including UV-visible, steady-state fluorescence, thermal fluorescence, circular dichroism (CD) spectroscopy along with Fourier transform infrared (FT-IR), dynamic light scattering (DLS) and enzymatic activity studies. These studies help the researcher develop better and new solvents to counteract the adverse effects of some ILs and enhance the properties of DESs and ILs, making them more biocompatible solvents for various biochemical processes.

2. Materials and methods

2.1. Materials

Commercially lyophilized powder of hen egg white lysozyme ($\geq 90\%$, ≥ 14 – 15 kDa) was procured from Sigma Aldrich, USA, while choline chloride (ChCl) and malonic acid were purchased from Aldrich with a purity of 99.5%. Ionic liquids, namely, 1-butyl-3-methylimidazolium chloride [BMIM]Cl and choline acetate [Chn][Ac], were obtained from Aldrich and had a high purity grade. Further, *Micrococcus lysodeikticus* (ATCC No. 4698) was also obtained from Sigma Aldrich for performing studies on enzyme activity.

2.2. Synthesis and characterization of DES and HIFs

2.2.1. Synthesis of choline-based deep eutectic solvent (DES). The DES was prepared by combining two economically and environmentally sustainable components,³⁵ *i.e.*, choline chloride (ChCl), a quaternary ammonium salt, which acts as an HBA, and malonic acid, which serves as an HBD. Here, the two components with a molar ratio [1:2] undergo mixing with constant stirring at about 80 °C for 1 h to attain a uniform liquid. The DES of ChCl with malonic acid is referred to as Maline.

2.2.2. Synthesis of hybrid ionic fluids (HIFs). To prepare HIFs, an equimolar ratio of IL and Maline (0.5 mol each) was mixed in a round-bottom flask. To obtain a homogenous solution of HIF, both components were heated at 80 °C with continuous stirring for 2 h.³⁵ Herein, two different HIFs were synthesized by combining DES Maline with IL [BMIM]Cl, forming HIF₁, while Maline on combining with [Chn][Ac] formed HIF₂. The characterization of the DES and HIFs was assessed by FT-IR spectroscopy.

2.2.3. Sample preparation. In this work, a 10 mM sodium phosphate buffer of pH 7 was prepared in double-distilled

deionized water with a resistivity of $18.3 \Omega \text{ cm}$ and was used to prepare all the samples. The stability of a protein was studied by incubating the protein samples (0.5 mg mL^{-1}) in a 2 mL screw-capped vial in different solvents, including DES, ILs and HIFs at varying concentrations, ranging from 0.1, 0.2, 0.3, 0.4 and 0.5 M for half an hour to attain equilibrium at 25°C . The protein concentration was fixed at 0.5 mg mL^{-1} for all the studies except for the DLS measurement, in which 1 mg mL^{-1} of protein concentration was employed. All the samples for the DLS measurements were filtered through a $0.2 \mu\text{m}$ pore size disposable syringe filter.

2.2.4. Fourier transform infrared (FT-IR) spectroscopic analysis of ILs, DES and HIFs. Infrared spectroscopy is a standard technique used for assessing liquid structures. The intra-molecular vibrational modes of ions constituting the materials are quite sensitive to their local potential environment. This technique is used to analyse the strength of hydrogen bond interaction and identify the structures of ILs, DES, and HIFs. FT-IR spectral responses are studied to understand the H-bonding between IL and DES through spectral shifts. The structural analysis of pure ILs [BMIM]Cl and [Chn][Ac], DES [Maline], and HIF₁ and HIF₂ were recorded by FT-IR under precise conditions at room temperature, and the spectra are displayed in Fig. 1.

The FT-IR spectrum in black represents an IL such as [BMIM]Cl; here, the peaks are observed at 1120 , 1415 and 1518 cm^{-1} , which resemble the peaks of $-\text{C}-\text{C}-\text{N}$, $-\text{CH}_2$ and component chloride, respectively. However, the red color shows the spectrum of another IL, [Chn][Ac], which shows three different peaks, one each at 1336 , 1432 and 1569 cm^{-1} , suggesting the presence of $-\text{OH}$ bending, $-\text{CH}_2$ and $\text{N}-\text{O}_{\text{str}}$, respectively. Furthermore, the FT-IR spectrum in blue represent the four spectral peaks of Maline, which shows a peak near 1219 cm^{-1} , which is for $\text{C}-\text{O}_{\text{str}}$, 1379 cm^{-1} , which resembles $\text{O}-\text{H}$ bending, though the peaks at 1479 and 1715 cm^{-1} suggest the presence of $\text{C}-\text{H}$ bending and $\text{C}=\text{O}_{\text{str}}$. FT-IR supported the new chemical environment developed in HIF₁ and HIF₂. As depicted in Fig. 1, On

comparing the [BMIM]Cl with HIF₁, the peaks are shifted: the $-\text{C}-\text{C}-\text{N}$ frequency is shifted from 1120 to 1169 cm^{-1} , while the peak of the chloride component is also shown to be shifted from 1518 to 1568 cm^{-1} . Similarly, for Maline to HIF₁ the wavenumber shifts from 1219 to 1229 cm^{-1} for the $\text{C}-\text{O}_{\text{str}}$ frequency, from 1379 to 1375 cm^{-1} for $\text{O}-\text{H}$ bending, and from 1715 to 1711 cm^{-1} for $\text{C}=\text{O}_{\text{str}}$. Meanwhile, 1219 , 1379 , 1479 and 1715 to 1236 , 1366 , 1482 and 1711 cm^{-1} for Maline to HIF₂ represent $\text{C}-\text{O}_{\text{str}}$, $\text{O}-\text{H}$ bending, $\text{C}-\text{H}$ bending and $\text{C}=\text{O}_{\text{str}}$, respectively; however, in contrast to [Chn][Ac], 1562 cm^{-1} was shifted to 1522 cm^{-1} , revealing $\text{N}-\text{O}_{\text{str}}$. The spectral frequency shifts in HIF₁ and HIF₂, in comparison to ILs and DES, support the formation of HIFs.³⁵

2.3. Methods

The experimental techniques used in the present study were explained in earlier work^{36,37} and are briefly described in ESI.†

3. Results and discussion

3.1. Spectroscopic studies of Lyz in the presence of ILs, DES and HIFs

The absorption spectra of Lyz in ILs, DES, and HIFs provide information about conformational changes, in particular revealing the variation in microenvironment, which generally results in modification in aromatic residues, such as phenylalanine (Phe), tyrosine (Try) and tryptophan (Trp). The absorption maximum for Lyz was observed at 280 nm , attributed to the $\pi-\pi^*$ transition of aromatic amino acid residue.³⁷ As depicted in Fig. S1(a)–(e) (ESI†), no peak shift was observed for Lyz in ILs, DES and HIFs, indicating no significant structural perturbation of the structure of Lyz. Fig. S1(a) and (b) (ESI†) show the absorption spectra of Lyz in ILs such as [BMIM]Cl and [Chn][Ac], indicating an increase in A_{max} . This may be attributed to reasonably unstable hydrophobic pockets of amino acid residues ascribed to electrostatic repulsion, leading to more exposure of these residues towards solvents. However, in the case of [BMIM]Cl, when the concentration of [BMIM]Cl increased from 0.1 to 0.5 M , the absorbance was found to be more enhanced (Fig. S1(a), ESI†). A decrease in absorbance with concentration was witnessed in the presence of [Chn][Ac] (Fig. S1(b), ESI†); but it was still higher than for pure Lyz. Thus, both [BMIM]Cl and [Chn][Ac] enhance absorbance, though the concentration-dependent trend was opposite between the two ILs. Moreover, the addition of [Maline] to Lyz again led to an increase in A_{max} (Fig. S1(c), ESI†), although the concentration trend was similar to [BMIM]Cl, *i.e.*, the absorbance increased with the concentration increasing from 0.1 to 0.5 M .

The absorption spectra of Lyz were also probed in the presence of HIFs, as depicted in Fig. S1(d) and (e) (ESI†). The absorption spectra of Lyz in HIF₁ (Fig. S1(d), ESI†) show an abrupt pattern, *i.e.*, at lower concentrations, A_{max} was found to be enhanced in contrast to native Lyz, while a decrease in absorbance, making it even less than its native form, was observed at higher concentration. Moving forward, Lyz, in the presence of HIF₂ (Fig. S1(e), ESI†), showed a decrease in absorbance in contrast to the native

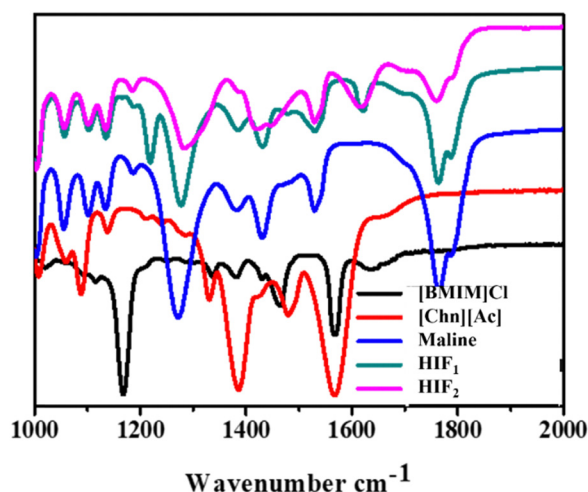


Fig. 1 FT-IR of ILs: [BMIM]Cl (black), [Chn][Ac] (red); DES: [Maline] (blue); and HIFs: HIF₁ (dark cyan) and HIF₂ (pink).

form of Lyz. As the concentration of HIF₂ increased from 0.1 to 0.4 M, A_{max} was found to be enhanced, though the absorbance remained less than that of Lyz in the buffer. However, at 0.5 M concentration, the absorbance was more reduced than when HIF₂ was increased from 0.1 to 0.4 M. This reduction in absorbance indicates decreased exposure of aromatic amino acid residues, namely Phe, Try and Trp, to a solvent, which leads to certain conformational changes in the native structure of Lyz due to its interaction with the studied biocompatible solvents. Moreover, Fig. 2(a) illustrates the comparative analysis of the impact of different solvents on Lyz at 0.3 M. Strikingly, the effect of ILs, Maline and HIF₁ on the absorbance of Lyz was almost similar, *i.e.*, enhanced A_{max} was observed while HIF₂ molecules surround the protein structure and minimize the exposure of aromatic amino acid residues to the solvent environment. Subsequently, the overall conclusion drawn was that the HIFs had overcome the deleterious effect caused by ILs and DES on Lyz.

Fluorescence emission spectra were studied in the same environment to gain deeper insight into the conformational stability of protein in ILs, DES, and HIFs. The fluorescence emission spectra of Trp residues in a protein are vulnerable to the polarity of the local environment of the fluorophores, which

is one of the major factors responsible for the decrease in the fluorescence intensity of Trp.²¹ The unfolding of the protein tends to broaden the spectrum due to the large variety of local environments of the fluorophores, which gives rise to different shifts in emission wavelengths. However, Lyz contains six Trp residues in various domains, two of which are Trp 62 and Trp 108, which are partially exposed to the co-solvents and behave as an intrinsic fluorescence probe.³⁸ Thus, changes in intrinsic fluorescence were employed to understand the conformational changes caused by incorporating the protein into the studied ILs, DES and HIFs in contrast to a buffer. Herein, Lyz in the buffer was excited at 290 nm, and the emission maximum (λ_{max}) was observed at 340 nm.³⁹ A small blue shift was observed in all the study systems in contrast to the buffer, as depicted in Fig. S2(a)–(e) (ESI[†]), which suggests the location of the Trp side chain in the lower polarity and higher homogeneity surroundings in comparison to a fully denatured environment where the emission spectrum shifted towards the red.²¹

Adding ILs to the protein leads to a substantial change in the emission spectra of Lyz (Fig. S2(a) and (b), ESI[†]). A sharp decrease in fluorescence intensity (I_{max}) was observed in the presence of both ILs, [BMIM]Cl and [Chn][Ac], also suggesting a

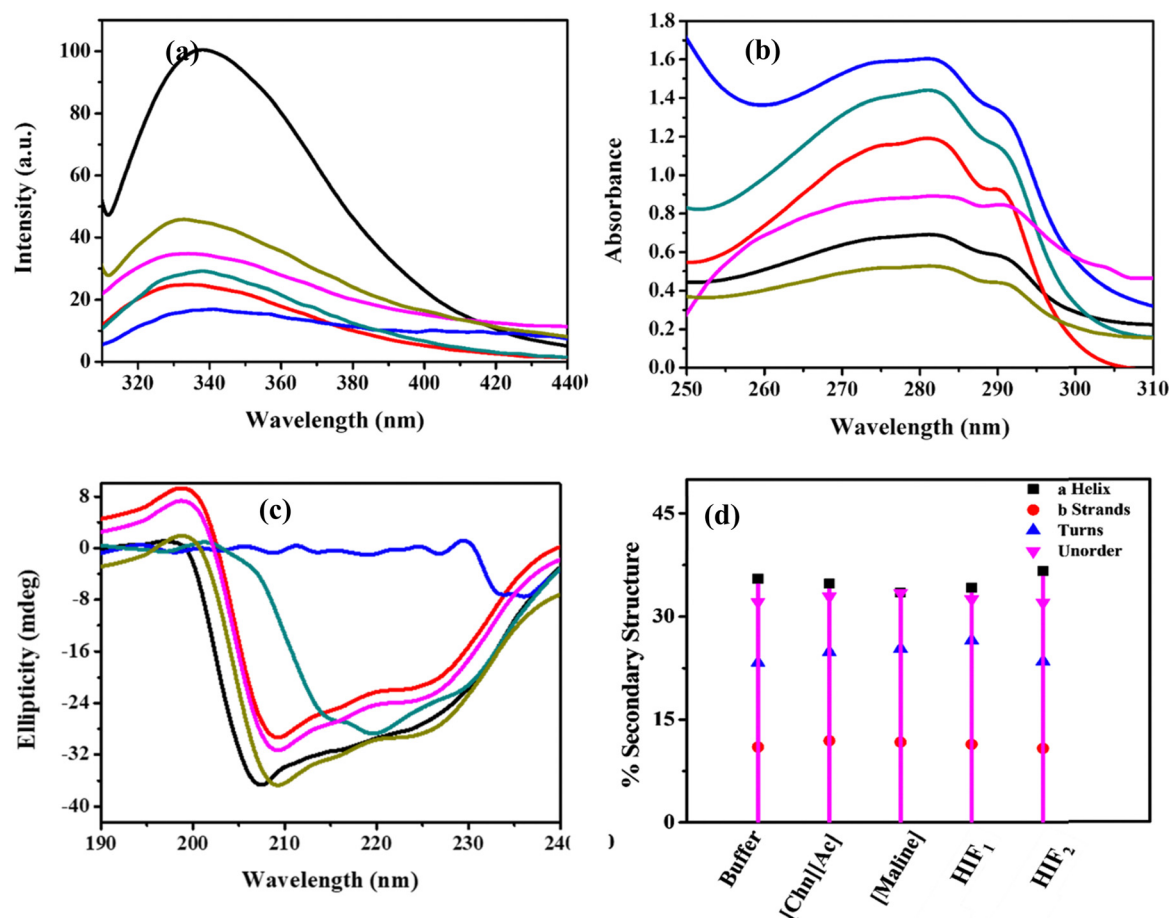


Fig. 2 Spectroscopic analysis: (a) UV-vis, (b) steady-state fluorescence, (c) far UV-CD of Lyz (0.5 mg mL⁻¹) in a buffer (black) and in the presence of 0.3 M of ILs: [BMIM]Cl (blue), [Chn][Ac] (dark cyan); DES: Maline (red); HIFs: HIF₁ (pink), HIF₂ (olive); and (d) % secondary structure of Lyz in the buffer and in the presence of 0.3 M of Maline, [Chn][Ac], HIF₁ and HIF₂; the secondary composition was not obtained for Lyz in [BMIM]Cl.

decrease in hydrophobicity around the Trp residues. Meanwhile, as the concentration of ILs increased from 0.1 to 0.5 M, the I_{\max} of Lyz was not significantly altered in either [BMIM]Cl or [Chn][Ac]. For Lyz in the presence of [Maline] (Fig. S2(c), ESI[†]), appreciable quenching of fluorescence was observed at all the studied concentrations of DES. Emission spectra were also probed for Lyz in the presence of HIFs, as illustrated in Fig. S2(d) and (e) (ESI[†]); a similar quenching trend was observed for the protein in HIF₁ (Fig. S2(d), ESI[†]) where the quenching effect was quite a bit less when analyzed in the presence of HIF₂ in contrast to ILs, DES and HIF₁. This quenching could be due to the exposure of the Trp residue to the biocompatible solvent or it may be due to the interaction of co-solvents with the functional groups of the protein; thus, the biocompatible solvents lead to a substantial change in the microenvironment of Trp residues, which are responsible for fluorescence quenching.

Additionally, Fig. 2(b) illustrates a comparative analysis of 0.3 M of different biocompatible solvents at a fixed concentration of Lyz (0.5 mg mL⁻¹). The biocompatible solvent induced quenching on the intrinsic fluorescence of Lyz, thus suggesting the presence of a novel green solvent which imparts an appreciable change to the microenvironment of Trp residues. In monitoring Fig. 2(b), the highest quenching was observed in [BMIM]Cl, while quite a lesser extent of quenching was observed in the case of HIF₂. As summarized from the steady-state fluorescence spectroscopy, the perturbation that occurred in or around the Trp moiety directly alters the secondary structure of Lyz; hence, the influence caused by the ILs and DES has been tuned by the HIFs. Therefore, it can be concluded that among ILs, DES, and HIFs, HIF₂ proved to be more biocompatible and maintained the conformational stability of Lyz.

CD spectroscopy was performed to obtain deeper insights and to comment on the extent and nature of protein-biocompatible solvents. Far UV-CD was employed to understand the alteration in the secondary structure, including α -helical and β -sheets of the protein due to folding and refolding, along with a quantitative estimation of the α -helical content of the protein.^{40,41} The CD spectra of Lyz exhibit two distinctively negative peaks due to the transition of the amide group of the peptide bond of the protein additives.^{40–42} Therefore, the two negative bands at 208 and 222 nm represent the π - π^* and n - π^* protein transition, respectively.³⁹ Fig. 2(c) portrays the far UV-CD analysis of Lyz at 0.3 M of all the studied biocompatible solvents. Fig. S3(a)–(e) (ESI[†]) represent the spectral curves of Lyz in the absence and presence of ILs, DES and HIFs, and it was noticed that the spectral shape of the CD signal does not change significantly in the presence of Maline, HIF₁ or HIF₂. However, the spectral shape is abruptly changed in the presence of [BMIM]Cl and [Chn][Ac]. Fig. S3(a) and (b) (ESI[†]) display the CD spectral curves in the presence of ILs such as [BMIM]Cl and [Chn][Ac]; the peaks at 208 and 222 nm vanished and diminished, which indicates the structural denaturation of the protein.⁴¹ Further, Fig. S3(c) (ESI[†]) depicts the far CD spectral curve of Lyz in the presence of Maline in which the negative ellipticities of Lyz for all the concentrations are quite a bit smaller than the native form of Lyz, indicating that

Maline has a stabilising influence on the secondary structure of Lyz. In the case of the HIFs, Fig. S3(d) and (e) (ESI[†]) suggest a similar pattern for the spectral curve and ellipticity in the presence of Maline. Interestingly, in HIF₂, the ellipticities are found to be more negative, at a concentration from 0.2 to 0.4 M in contrast to the buffer, while at 0.1 M and 0.5 M, the CD spectral ellipticities are similar to those in Maline and HIF₁. The study mentioned above intimates the secondary structural stabilisation of Lyz in the presence of the HIFs.

DICROWEB online was employed to estimate the variation in the secondary structure of Lyz in the absence and presence of biocompatible solvents. Fig. 2(d) represents the percent secondary structure at 0.3 M, while the concentration-dependent effect of these co-solvents on the secondary structure of Lyz is exemplified in Fig. S4(a)–(d) (ESI[†]). The values of α -helical, β -sheets, turns, and unordered composition of the native form of Lyz in a buffer at pH = 7 were found to be 35.5%, 11%, 23.3% and 32.1%, respectively, which reveals good agreement with the literature.⁴³ However, due to the diminished characteristic peak of Lyz in [BMIM]Cl, the secondary structure composition was not procured. In observing Fig. 2(d), a major variation in the composition of the secondary structure of Lyz was observed in the presence of [Chn][Ac], Maline and HIF₁; the α -helical component was found to slightly decrease to 33.9% in [Chn][Ac], 33.4% in Maline, 34.5% in HIF₁. However, β -sheets were found to be slightly increased in [Chn][Ac] (12.2%), Maline (11.8%) and HIF₁ (11.7%). In addition to this, the turns and unordered content were also found to be higher than in the native form, *i.e.*, 25%, 25.4% and 27.9% turns for [Chn][Ac], Maline and HIF₁, respectively, while the unorderedness was found to be up to 33.9%, 33.4% and 32.5% for [Chn][Ac], Maline, and HIF₁, respectively. This indicates the negative impact of these biocompatible solvents, such as [Chn][Ac], Maline and HIF₁, towards the stability of the protein. Interestingly, HIF₂ boosted the α -helical protein content up to 37%, decreasing the β -content and unorderedness to 10.5% and 32%, respectively. Therefore, the comparative analysis of both HIFs illustrates that HIF₂ provides more secondary structural intactness than HIF₁. These results agree well with the results obtained from far UV-CD.

3.2. Fourier transform infrared (FT-IR) spectroscopic studies of Lyz in the presence of ILs, DES and HIFs

FT-IR spectroscopy was employed to gain a deep understanding of the secondary structure of a protein in the absence and presence of biocompatible solvents such as ILs, DES and HIFs. This technique is sensitive to secondary structure and represents the two-absorption bands for a protein conventionally termed amide I and amide II at wavenumbers 1700–1600 cm⁻¹ and 1600–1500 cm⁻¹, respectively. Amide I commonly characterises the secondary structure of a protein due to the C=O stretching vibration of the peptide bond that helps to regulate the secondary structure (α -helical and β -sheets) of Lyz. The spectral contribution leads to a broad band with overlapping subspectra.⁴³ Fig. 3 portrays the representative change in the FT-IR secondary structure of Lyz in the buffer and in 0.3 M of ILs, DES and HIFs. In Fig. 3, the spectra of Lyz in the buffer are significantly changed in the presence of biocompatible solvents. Herein, in

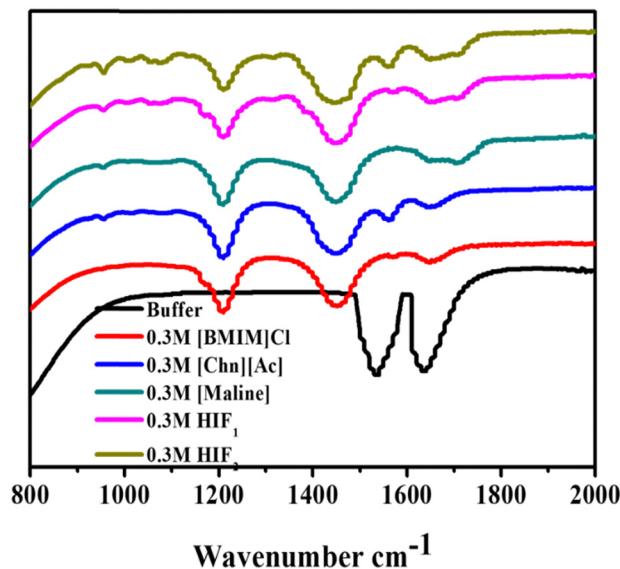


Fig. 3 FT-IR spectroscopic analysis of Lyz (0.5 mg mL⁻¹) in buffer (black) and in the presence of 0.3 M of ILs: [BMIM]Cl (red), [Chn][Ac] (blue); DES: [Maline] (dark cyan); HIFs: HIF₁ (pink), HIF₂ (olive).

the black-coloured spectra, peaks between 1700 cm⁻¹ and 1600 cm⁻¹, and between 1600 cm⁻¹ and 1500 cm⁻¹ were observed, reflecting the presence of amide I and amide II bands. Additionally, upon further observation of the spectra, the addition of all studied solvents led to a change in the secondary structure of Lyz: the amide I and amide II bands of the protein became smaller, and new peaks arose.

As depicted in Fig. 3, the addition of [BMIM]Cl into Lyz leads to the rise of three peaks. Among them, two shifted peaks at 1214 cm⁻¹ and 1450 cm⁻¹, representing C-H bending and C-O_{str}, may be due to the intermolecular interaction of [BMIM]Cl and Lyz, while one peak between 1700 cm⁻¹ and 1600 cm⁻¹ was also observed to show the presence of an amide I band, which may be due to the intermolecular interaction of [BMIM]Cl and Lyz.

Nevertheless, Lyz in the presence of [Chn][Ac] shows three shifted peaks in contrast to [Chn][Ac] and native Lyz; the peaks are at 1214 cm⁻¹ (O-H bending), 1446 cm⁻¹ (-CH₂) and 1565 cm⁻¹ (amide II). Further, the addition of Maline to Lyz again leads to three shifted peaks: one at 1206 cm⁻¹ shows O-H bending, while a peak at 1446 cm⁻¹ represents C-H bending, whilst one broad peak between 1642 cm⁻¹ and 1711 cm⁻¹ shows resemblance to the amide I band. On the other hand, when observing Fig. 3, HIF₁ in Lyz reveals one peak at 1196 cm⁻¹, representing the -C-C-N frequency. However, the peak at 1453 cm⁻¹ suggests C-H bending and a broad peak between 1653 cm⁻¹ and 1714 cm⁻¹ reveals the presence of an amide I band. Interestingly, four peaks were observed in Lyz in the presence of HIF₂: at 1203 cm⁻¹ for C-O_{str}, at 1446 cm⁻¹ for C-H bending, at 1558 cm⁻¹ N-O_{str}, and a broad small peak between 1653 cm⁻¹ and 1714 cm⁻¹ represents the presence of amide I. However, the peaks of amide I and amide II were weaker in the presence of all the studied solvents than in the buffer.

Furthermore, in conclusion, the exposure of Lyz to all the considered biocompatible solvents revealed more or less similar significant changes, which suggests the solvent may disrupt the local environment due to the exposure of amino acid residue to the co-solvent, which leads to intermolecular interactions between them.

3.3. Thermal stability analysis of Lyz in the presence of ILs, DES and HIFs

Temperature plays a vital role in the stability and activity of a protein. Hence, we also studied the thermal stability of Lyz in the absence and presence of biocompatible co-solvents. However, to evaluate the thermal stability of the protein, the change in the transition temperature (T_m) was determined using thermal fluorescence spectroscopy, which helps to describe the thermal unfolding of Lyz. The T_m values for Lyz in [BMIM]Cl, [Chn][Ac], Maline, HIF₁, and HIF₂ as a function of concentration are depicted in Fig. 4 and collected in Table S1 (ESI[†]), while the thermal transition curves of Lyz in the above-mentioned solvents are reported in Fig. S5(a)–(e) (ESI[†]). The T_m value of the native structure of Lyz was found to be 70.87 °C, which correlates well with the available literature.³⁷ On observing Fig. 4 and Table S1 (ESI[†]), we perceive that the T_m of Lyz in [BMIM]Cl were found to be lower than the value in the native state. But, intriguingly, T_m was found to be higher only at 0.1 M. It was also noticed that as the concentration of [BMIM]Cl increased, the T_m values decreased, which suggests that the higher concentration of IL destabilises the protein structure. However, the T_m values of Lyz in [Chn][Ac] were found to be higher than for Lyz in buffer at all the studied concentrations while, with the rise in the concentration of [Chn][Ac], the values were slightly decreasing. This illustrates that [Chn][Ac] thermally stabilises the native structure of Lyz. In other words, the addition of Maline shows a drastic fall in the T_m value of Lyz with concentration, revealing that Maline disrupts the structure of Lyz and leads to destabilisation in the confirmation of the protein.

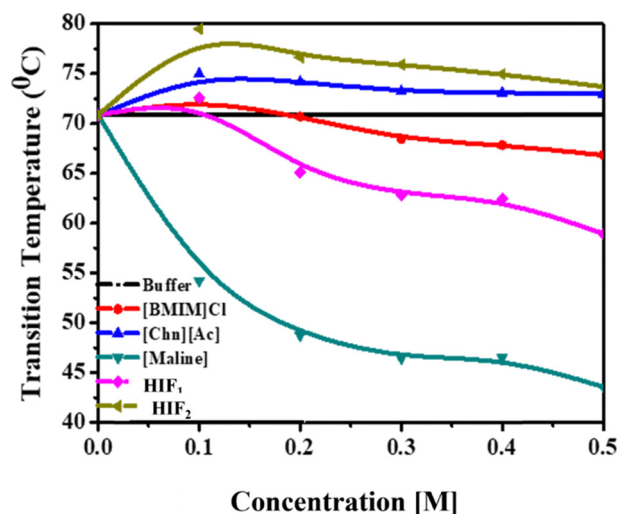


Fig. 4 Transition temperature of Lyz (0.5 mg mL⁻¹) in buffer (black) and in the presence of varying concentrations of ILs: [BMIM]Cl (red), [Chn][Ac] (blue); DES: [Maline] (dark cyan); and HIFs: HIF₁ (pink), HIF₂ (olive).

Conversely, upon the addition of HIF₁ to Lyz, the T_m values were pronounced only at 0.1 M ($T_m = 72.62$ °C) whereas, as the concentration increased from 0.2 to 0.5 M, the T_m values were found to be lower than that of pure protein, which may suggest that only at 0.1 M, is the effect of IL distinct; at 0.1 M, the T_m of Lyz in [BMIM]Cl was reported as 72.49 °C in contrast to Maline ($T_m = 54.25$ °C). Altogether, upon observing Fig. 4 and Table S1 (ESI[†]), [BMIM]Cl thermally stabilises the structure of Lyz at lower concentrations, while DES leads to destabilisation at all concentrations of Maline. Interestingly, the results of Fig. 4 explicitly elucidate that HIF₂ drastically enhanced the thermal stability of Lyz at all the studied concentrations, though it was found to be reduced at higher concentrations of HIF₂; however, it was still found to be higher than that in the buffer as well as in the ILs and DES. The reported T_m for HIF₂ ranged from 73.69 to 78.48 °C while in the case of their parent component, that is [Chn][Ac], the T_m values were found between 72.96 to 74.97 °C and in Maline, it fluctuated between 43.57 and 54.25 °C, which are much lower than the T_m value of native Lyz. Therefore, we suggest that [Chn][Ac] intensifies the properties of HIF₂ over Maline and stabilises the structure of Lyz. Thus, the combination of [Chn][Ac] and Maline leads to tremendous properties in HIF₂ compared to [BMIM]Cl and Maline in HIF₁. Therefore, the novel HIF₂ intensifies the thermal stability of native Lyz in

comparison to ILs and DES, as the formation of HIFs counters the negative effects of either DES.

Hence, based on the observations of Table S1 (ESI[†]), one can conclude that the effect of the HIFs on thermal stability was highly concentration-dependent. Fascinatingly, these results illustrate that [BMIM]Cl, Maline and HIF₁ lowered the T_m value while [Chn][Ac] and HIF₂ displayed elevated T_m values, emphasising that thermal stability has to be induced in the structure of Lyz by these solvents, where we observed the pronounced effect of ILs over Maline in the HIFs.

The thermal unfolding mechanism of a protein can be understood by studying various thermodynamic parameters, such as the Gibbs free energy change of unfolding (ΔG_u), and the changes in entropy (ΔS_m), enthalpy (ΔH_m) and heat capacity (ΔC_p), which are acquired from the standard thermodynamic profile,³⁹ as reported in ESI[†]. The changes in the thermodynamic parameters of Lyz in the absence and presence of co-solvents are displayed in Fig. 5(a–d), and Table S2 (ESI[†]) summarizes all the thermodynamic factors related to the stability of Lyz in the presence of the studied co-solvents (ILs, DES and HIFs). A positive value of ΔG_u signifies the native state of Lyz, whereas a negative value signifies the denatured state.⁴⁴ The values of ΔG_u and ΔH_m of the protein in its native state were 3.63 and 65.36 kJ mol^{−1}, respectively. On monitoring

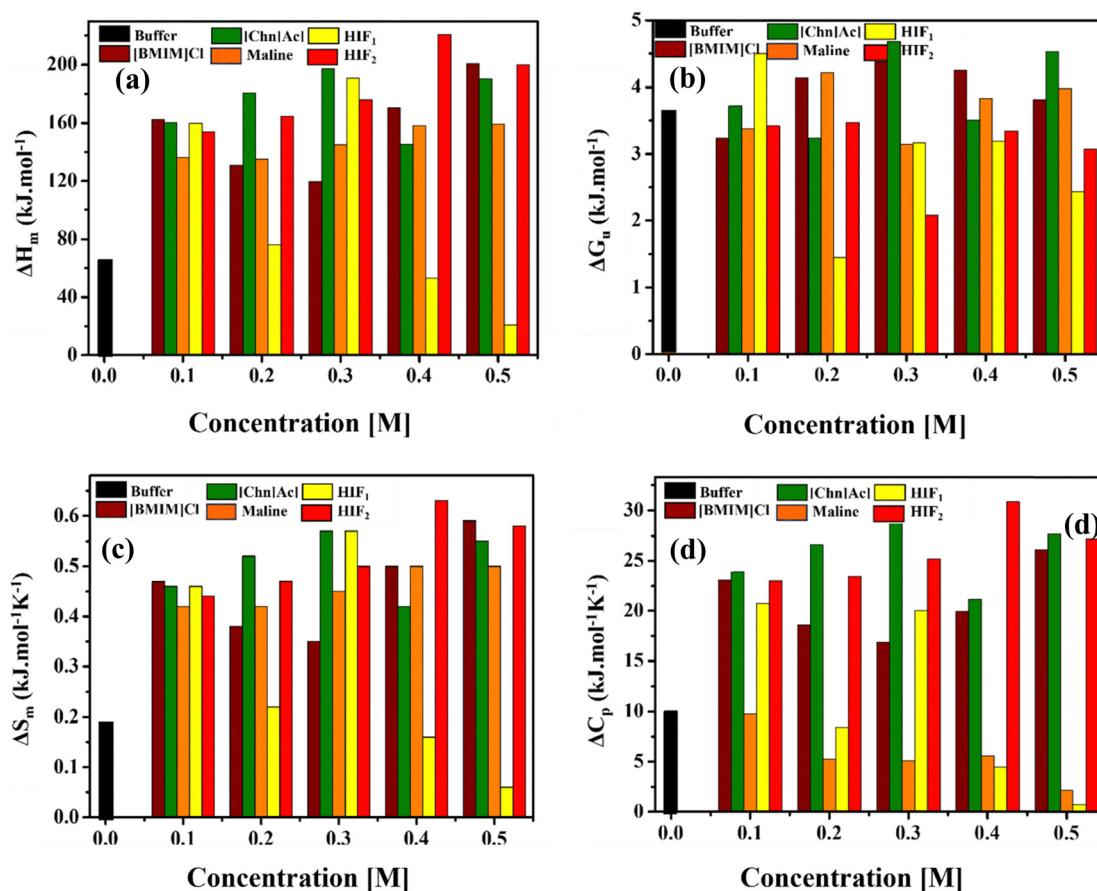


Fig. 5 Thermodynamic parameters, (a) Gibbs free energy, (b) enthalpy (c) entropy and (d) heat capacity, of Lyz (0.5 mg mL^{−1}) in buffer and in the presence of varying concentrations of ILs: [BMIM]Cl, [Chn][Ac]; DES: [Maline]; and HIFs: HIF₁, HIF₂.

Fig. 5(a), the ΔG_u values of Lyz in [BMIM]Cl were found to first decrease and then increase at higher concentrations, except at 0.5 M of [BMIM]Cl. In contrast to this, the values of ΔG_u of Lyz in the presence of [Chn][Ac] and Maline were not found to follow an appropriate trend. However, the ΔG_u values in the presence of HIF₁ were found to be lower than the value of ΔG_u in its native state except at 0.2 M, whereas, in HIF₂, the value of ΔG_u was observed to be slightly lower than its native form (3.63 kJ mol⁻¹).

Fig. 5(b and c) illustrate the variations in ΔH_m and ΔS_m in the presence of all the studied co-solvents at all concentrations (0.1–0.5 M). It is observed that the values of ΔH_m and ΔS_m in ILs, Maline and HIF₂ reveal an increasing trend except at 0.4 M of [Chn][Ac], which shows quite a decrease in the values of ΔH_m and ΔS_m ; while Lyz in HIF₁ demonstrates no particular trend, and at a higher concentration of HIF₁ the values of ΔH_m and ΔS_m are found to be lower than for native protein. This suggests that Lyz in HIF₁ shows an unfavourable interaction between the functional group of the protein and the solvent, whereas ILs, Maline and HIF₂ interfere with the functional moiety of the protein, leading to its unfolding. In addition to the above-mentioned thermodynamic parameters, ΔC_p play an essential role in determining the energetics of the structural stabilisation of the native protein.^{44–46} Normally, protein unfolding is accompanied by a positive value of ΔC_p , which is a maximum for stability of its native structure with marked ramifications for ΔG_u .^{44,45} Fig. 5(d) displays the ΔC_p of Lyz in the presence of different solvents as a function of their concentration. The calculated ΔC_p value was 10.04 kJ mol⁻¹ for the thermal unfolding of Lyz. In the case of Lyz in [BMIM]Cl, it is observed that at an initial concentration (0.1 M), there was a rise in the values of ΔC_p and then they decreased and remained constant up to 0.3 M of IL. After this, the value was again raised with a higher concentration of [BMIM]Cl. The value of ΔC_p in [Chn][Ac] first increased, and then remained constant.

On the other hand, the ΔC_p of Lyz in Maline tended to decrease as the concentration increased, which indicates lower solvation of the hydrophobic core of the native structure of Lyz. Moreover, no particular trend was found in the presence of HIF₂. The value of ΔC_p was found to be high at 0.1 M, then it decreased and then again increased at 0.3 M, whereas in HIF₂, the value of ΔC_p was found to rise at all concentrations. These results are consistent with other obtained thermodynamic results. The overall conclusion is that HIF₂ enhances the conformational thermal stability of Lyz, which indicates [Chn][Ac] offsets the Maline (DES) and intensifies the thermal stability of the protein.

3.4. Dynamic light scattering (DLS) analysis of Lyz in the presence of ILs, DES and HIFs

To elucidate the aggregation size, we studied the variation in hydrodynamic diameters (d_H) of Lyz in the presence of ILs, DES and HIFs, and the data are presented in Fig. 6 and Fig. S6(a)–(e) (ESI[†]). The d_H for native Lyz in buffer was found to be 3.8 nm at 25 °C, consistent with the available literature.⁴⁷ The d_H value of Lyz in the presence of varying concentrations of biocompatible

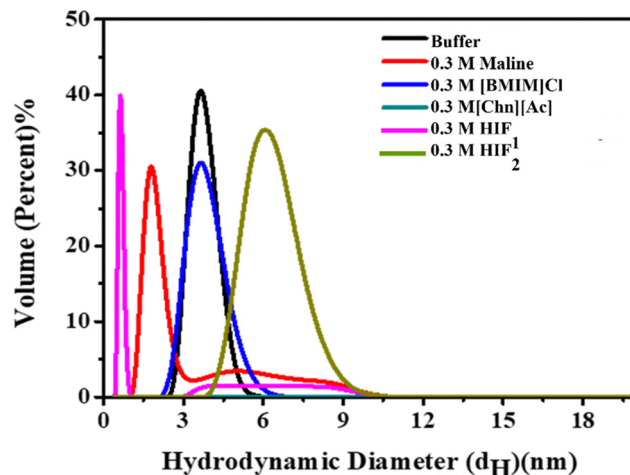


Fig. 6 Volume percent graph of DLS measurement of Lyz (0.5 mg mL⁻¹) in buffer (black) and in the presence of 0.3 M of ILs: [BMIM]Cl (blue), [Chn][Ac] (dark cyan); DES: [Maline] (red); and HIFs: HIF₁ (pink) and HIF₂ (olive).

solvents is tabulated in Table S3 (ESI[†]), where the presence of ILs leads to a rapid increase in protein size, which is attributed to the unfolding or aggregation of protein molecules (Fig. S6(a) and (b), ESI[†]). For DES (Fig. S6(c), ESI[†]) a similar trend was observed for variation in d_H only at lower concentrations (0.1 M and 0.2 M), while at higher concentrations, i.e., 0.3 M and 0.4 M, the size was found to be reduced, whereas a rapid increase in size was again observed at 0.5 M. Furthermore, a similar trend in size was also observed in Lyz–HIF₁, as depicted in Fig. S6(d) (ESI[†]), and here the size was very close to that of native Lyz at 0.1 M. Additionally, the d_H in HIF₂ reveals that at 0.2 M and 0.4 M, the size of the protein particle is quite close to that of native Lyz. However, the d_H values were higher than the native conformation for the rest of the concentrations (0.1, 0.3 and 0.5 M). Overall, ILs enhance the d_H of Lyz due to the formation of aggregates. However, no significant change was observed in the presence of DES at all studied concentrations. While HIFs can counteract the effect caused by ILs on the protein, as in HIF₂, the d_H values were found to be less than those of their parent ILs and close to the native conformation at some concentrations.

Altogether, the results enumerate that the effects of those co-solvents on Lyz ILs is devoid of any functional group, thus causing deleterious effects on the Lyz structure and stability. While DES also caused substantial perturbation to the structure of the protein. Interestingly, the mixture of ILs and DES leads to the formation of HIFs, causing marked stabilisation of the protein, as reflected in the DLS measurements in the spectroscopic studies.

3.5. Proteolytic activity of Lyz in of DES, ILs and HIFs

To elucidate the feasibility of prolonged enzyme storage, the enzymatic activity of Lyz was studied in the presence of ILs, DES and HIFs using *Micrococcus lysodeikticus* as a substrate and displayed in Fig. 7 and Fig. S7 (ESI[†]). Herein, the activity was

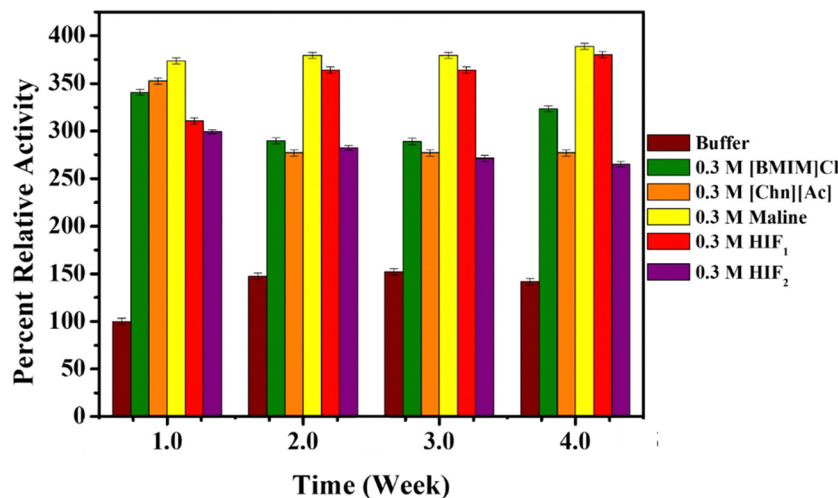


Fig. 7 Percent relative enzyme activity at different time intervals (in weeks) of Lyz (0.5 mg mL^{-1}) in buffer (orange) and at 25°C in the presence of 0.3 M of ILs: [BMIM]Cl (green), [Chn][Ac] (light blue); DES: [Maline] (yellow); and HIFs: HIF₁ (pink), HIF₂ (grey).

performed on the 1st day, 8th day (week 2), 16th day (week 3) and 24th day (week 4), and the values are tabulated in Table S4 of ESI†. Interestingly, the enzymatic activity of Lyz was enhanced in the presence of ILs, DES, and HIFs, compared to Lyz in the buffer (Table S4, ESI†). Moreover, the proteolytic activity of Lyz also increased with increasing concentration of [BMIM]Cl, Maline, HIF₁ and HIF₂ whereas in the presence of [Chn][Ac], the percent relative activity was more or less constant, as depicted in Fig. S7(a) (ESI†). Later, the enzymatic activity was obtained again on the 8th day (week 2) (Fig. S7(b), ESI†). The activity showed a slight decrease and followed a similar trend with concentration, in contrast to the 1st day (week 1) in the presence of ILs, Maline, or HIF₂ and at lower concentrations of HIF₁. Interestingly, the enzymatic activity in HIF₁ increased slightly with an increase in the concentration of HIF₁. Furthermore, on the 16th day (week 3) (Fig. S7(c), ESI†), the activity of Lyz in buffer was found to be slightly increased; however, for the enzymatic activity in the presence of ILs, DES and HIFs, the percent relative activity increased as a function of concentration and more enhanced activity was observed in the cases of Maline and HIF₁ of ~ 1.58 fold and 1.42 fold, respectively. Moreover, for the percent relative activity on the 24th day (week 4) (Fig. S7(d), ESI†), the activity was observed to increase slightly in contrast to the 16th day (week 3), and it also increased as the concentration of the studied solvents increased.

From Table S4 (ESI†), Maline (DES) and HIF₁ suggest majorly enhanced enzymatic activity compared to ILs and HIF₂ as a function of time and concentration. Therefore, this suggests that Maline and HIFs provide prolonged storage for the enzyme compared to ILs. Fig. 7 represents the activity of Lyz at 0.3 M of all the biocompatible co-solvents as a function of time. From Fig. 7 and Table S4 (ESI†), ~ 0.9 – 2.5 -fold increase in enzymatic activity of Lyz with time interval was observed in the presence of [BMIM]Cl and [Chn][Ac]. Moreover, ~ 1.74 – 2.5 -fold increased activity (from the 1st day (week 1) to the 24th day (week 4)) was also found in the presence of Maline. However, in the case of

HIF₁, the enzymatic activity was found to be ~ 1.68 – 2.10 fold higher than a native form of the enzyme when moving towards the 4th week, while HIF₂ represents ~ 0.86 – 2 -fold enhanced proteolytic activity of Lyz. Taken together, maline and HIFs provide better storage for the enzyme.

The majority of findings obtained from spectroscopic studies, DLS, and the enzymatic activity of Lyz suggest that the novel HIFs stabilise the Lyz structure and intensify the enzymatic activity. In the present study, ILs had quite a disturbance effect, while DES significantly perturbs the structure of the native protein, whereas HIFs (the combination of IL and DES) enhance the stability and activity of Lyz. Intriguingly, the enzymatic activity of Lyz is also boosted even after weeks of incubation in the presence of all co-solvents. HIFs behave as a significantly biocompatible solvent for Lyz. Between the two HIFs, HIF₂ is one of the most promising co-solvents for stabilising and enhancing the properties of native Lyz. Later, Maline, [Chn][Ac] also preserves the activity of Lyz while [BMIM]Cl destabilises the native state of Lyz; hence it perturbed the structural and thermal stability of the protein. Upon analysing the above-mentioned studies, [BMIM]Cl manifests a perturbation effect on the conformation of Lyz, which may be due to the formation of hydrogen bonds with amino acid residues of Lyz and ions of ILs. On the other hand, [Chn][Ac] perpetuates the structural integrity to a certain extent. However, DES (composed of 1 : 2 choline chloride and Maline) escalated the structural stability and activity of the protein.

Interestingly, HIFs reveal the enhanced activity and stability of the protein. DES preserves activity even after a month of incubation; in contrast, HIFs provide stability to the native structure of Lyz and escalate the activity due to the protective property of Maline, which shows domination over the perturbative nature of [BMIM]Cl. Moving forward, HIF₂ also enhances the structural stability and activity of Lyz because both IL and DES, such as [Chn][Ac] and Maline, provide stability to the protein along with enhanced activity. Although in terms of

activity, HIF₁ has a more pronounced effect than HIF₂, other studies reveal that HIF₂ intensifies the stability and activity of Lyz. Therefore, the interpretation is drawn that the newly synthesised HIFs show intensified properties over the limitations of the individual components. Thus, one can say that HIFs provide better biocompatibility for the protein in contrast to the individual constituents (ILs and DES), which shows good agreement with the literature³⁴ in which DES (1 : 2 ChCl:glycerol) and HIF ([EMIM]Cl and ChCl:glycerol) stabilise and preserve the native structure of stem bromelain. This represents an advanced and feasible way of packaging a protein with improved stability and activity, imparting schematic and robust bio-catalysis.

Hybrid ionic fluids, which are a combination of both an ionic liquid and a deep eutectic solvent, have been found to enhance the activity and stability of proteins compared to the individual constituents. A probable reason may be attributed to the synergistic effects, tuneable properties, enhanced solvation, and reduced protein denaturation offered by this unique combination of properties that these hybrid fluids possess. Thus, this work is intended to provide a scope of applications for eco-friendly solvents for proteins and promising sustainable alternatives for stabilising proteins and various biotechnological applications of enzymes.

4. Conclusions

The present work reports the remarkable potential of HIFs, which overcome the limitations of the individual components and act as alternative, greener, biocompatible solvent media for a native protein structure. This work also provides a comparative analysis of Lyz in the presence of ILs, DES and HIFs. Herein, the investigated biocompatible solvents are ILs such as [BMIM]Cl and [Chn][Ac], while the DES was composed of choline chloride as an HBA and malonic acid as an HBD, and HIFs such as [BMIM]ClMaline and [Chn][Ac]Maline. From spectroscopic and thermodynamic analysis, it was found that the HIFs behave as a significant biocompatible solvent for Lyz, and among them, HIF₂ is the most promising, followed by HIF₁, Maline, and [Chn][Ac], while [BMIM]Cl disturbs the native state of Lyz. Conversely, in the early weeks of incubation (1st day (1st week) and 8th day (2nd week)), the enzymatic activity tends to increase with an increase in the concentration of ILs, then it starts decreasing after the 16th day (3rd week) of incubation. In contrast, in DES, the spectroscopic results, particularly those from far UV-CD, suggest that the DES intensified the structural stability of Lyz and the enzymatic activity also increased with the concentration of DES, even after the 24th day (4th week) of incubation. Interestingly, the results acquired for the HIFs reveal that they enhance the structural stability and enzymatic activity of Lyz even after incubation. Moreover, the FTIR studies supported the results obtained from other spectroscopic analyses, suggesting that [Chn][Ac] and HIF₂ significantly protect the native structure of Lyz. Comprehensively, as a biocompatible solvent, it opens a way to recognise the role of novel HIFs for providing protein stability and potential, eco-friendly prolonged storage for Lyz. The present study also

suggests that HIF₂ is a more biocompatible solvent for protein structure than HIF₁. Therefore, one cannot conclude that all HIFs are biocompatible solvents for the native structure of proteins; hence, more studies are essential to come to fundamental conclusions about the native structure of a protein.

Conflicts of interest

There are no conflicts to declare.

Acknowledgements

We gratefully acknowledge the Council of Scientific & Industrial Research (CSIR), New Delhi, India through Grant No. 01/3016/21/EMR-II and University Grant Commission (UGC), New Delhi, India through Grant F.4-2/2006 (BSR)/CH/20-21/0112 for their financial support.

References

- 1 J. P. Mann, A. M. Cluskey and R. Atkin, *Green Chem.*, 2009, 785–792.
- 2 Q. Han, K. M. Smith, C. Damanin, T. M. Ryan, C. J. Drummond and T. L. Greaves, *J. Colloid and Interface Sci.*, 2021, 433–443.
- 3 R. A. Kumar, C. J. Drummond and T. L. Greaves, *Front. Chem.*, 2019, 1–11.
- 4 N. Gull, M. Ishtikhar, M. S. Alam, S. N. S. Andrabi and R. H. Khan, *RSC Adv.*, 2017, 28452–28460.
- 5 S. Mangialardo, L. Gontrani, F. Leonelli, R. Caminiti and P. Postorino, *RSC Adv.*, 2012, 12329–12336.
- 6 D. Rozema and S. H. Gellman, *J. Biochem.*, 1996, 15760–15771.
- 7 U. K. Singh, M. Kumari, S. H. Khan, H. B. Bohidar and R. Patel, *ACS Sustainable Chem. Eng.*, 2018, 803–815.
- 8 C. Schröder, *Top. Curr. Chem.*, 2017, 1–26.
- 9 P. M. Reddy, P. Umapathi and P. Venkatesu, *Phys. Chem. Chem. Phys.*, 2015, 184–190.
- 10 J. V. Rodrigues, V. Prosineeki, I. Marrucho, L. P. N. Rebelo and C. M. Gomes, *Phys. Chem. Chem. Phys.*, 2011, 13614–13616.
- 11 S. Nandi, S. Purui, R. Halder, B. Jana and K. Bhattacharyya, *Biophys. Rev.*, 2018, 757–768.
- 12 D. Constatinescu, C. Herrmanna and H. Weingartner, *Phys. Chem. Chem. Phys.*, 2010, 1756–1763.
- 13 K. Fujita, D. R. MacFarlane and M. Forsyth, *Chem. Commun.*, 2005, 4804–4806.
- 14 C. Lange, G. Patil and R. Rudolph, *Protein Sci.*, 2005, 2693–2701.
- 15 N. Byrne, L. M. Wang, J. P. Belieres and C. A. Angell, *Chem. Commun.*, 2007, 2714–2716.
- 16 N. Yadav and P. Venkatesu, *Phys. Chem. Chem. Phys.*, 2022, 13474–13509.
- 17 E. Durand, J. Lecomte, B. Baréa and P. Villeneuve, *J. Process Biochem.*, 2012, 2081–2089.
- 18 D. Lindberg, M. de La Fuente Revenga and M. Widersten, *J. Biotechnol.*, 2010, 169–171.
- 19 H. Zhao, G. A. Baker and S. Holmes, *J. Mol. Catal. B: Enzym.*, 2011, 163–167.

- 20 E. Durand, J. Lecomte and P. Villeneuve, *Eur. J. Lipid Sci. Technol.*, 2013, 379–385.
- 21 R. Esquembrea, M. Jesus, J. Sanza, G. Wallb del Montec, F. R. Mateo and M. L. Ferrer, *Phys. Chem. Chem. Phys.*, 2013, 11248–11256.
- 22 A. A. Shamsuri, *Makara Sci. Ser.*, 2011, 101–106.
- 23 A. Stark, P. Behrend, O. Braun, M. Anja and J. Rank, *Green Chem.*, 2008, 1152–1161.
- 24 T. Phuong, T. Pham, C. Cho and Y. Yun, *Water Res.*, 2010, 352–372.
- 25 J. C. Thermodynamics, P. K. Chhotarray and R. L. Gardas, *J. Chem. Thermodyn.*, 2014, 117–124.
- 26 G. Chatel, J. F. B. Pereira, V. Debbeti, H. Wang and R. D. Rogers, *Green Chem.*, 2014, 2051–2083.
- 27 H. Wang, S. P. Kelley, J. W. Brantky, G. Chatel, J. Shamshina, J. F. B. Pereira, V. Debbeti, A. S. Myerson and R. D. Rogers, *Phys. Chem. Chem. Phys.*, 2015, 993–1002.
- 28 K. Huang, F. F. Chen, D. J. Tao and S. Dai, *Curr. Opin. Green Sustainable Chem.*, 2017, 67–73.
- 29 S. H. Lian, C. F. Song, Q. L. Liu, E. H. Duan, H. W. Ren and Y. Kitamura, *J. Environ. Sci.*, 2021, 281–298.
- 30 H. Maka, T. Sychaj and K. Kowalczyk, *J. Appl. Polym. Sci.*, 2014, 40401–40407.
- 31 M. K. Banjare, K. Behera, M. L. Satnami, S. Pandey and K. K. Ghosh, *RSC Adv.*, 2018, 7969–7979.
- 32 O. Lanaridi, S. Platzer, W. Nischkauer, A. Limbeck, M. Schnurch and K. A. Bica-Schroder, *Molecule*, 2021, 7204–7219.
- 33 T. Wang, Q. Guo, P. Li and H. Yang, *Food Chem.*, 2022, 133225–133232.
- 34 S. Nakka, A. Sindhu, D. Chahar, M. Bisht, N. Devunuri and P. Venkatesu, *ACS Sustainable Chem. Eng.*, 2023, 6395–6404.
- 35 P. K. Chhotarray, S. K. Biswal and S. Pandey, *J. Mol. Liq.*, 2020, 113477–113483.
- 36 D. Dhiman, M. Bisht, A. P. M. Tavares, M. G. Freire and P. Venkatesu, *ACS Sustainable Chem. Eng.*, 2022, 5404–5420.
- 37 I. Jha, A. Rani and P. Venkatesu, *ACS Sustainable Chem. Eng.*, 2017, 8344–8355.
- 38 J. Mathew and K. Usha, *J. Adv. Sci. Res.*, 2022, 89–95.
- 39 M. Bisht, A. Kumar and P. Venkatesu, *Int. J. Bio. Macromol.*, 2015, 1074–1081.
- 40 M. Kumari, P. Kumari and H. K. Kashyap, *Phys. Chem. Chem. Phys.*, 2022, 5627–5637.
- 41 J. Parnica and M. Antalík, *J. Mol. Liq.*, 2014, 23–26.
- 42 S. Barik, A. Mahapatra, N. Preeyanka and M. Sarkar, *Phys. Chem. Chem. Phys.*, 2023, 20093–20108.
- 43 K. Chaudhary, N. Yadav, P. Venkatesu and T. D. Masram, *ACS Appl. Bio Mater.*, 2021, 6112–6124.
- 44 N. Yadav, K. Bhakuni, M. Bisht, I. Bahadur and P. Venkatesu, *ACS Sustainable Chem. Eng.*, 2020, 10151–10160.
- 45 A. Rani and P. Venkatesu, *Int. J. Biol. Macromol.*, 2015, 189–201.
- 46 A. Sindhu, N. K. Mogha and P. Venkatesu, *Int. J. Biol. Macromol.*, 2019, 1–10.
- 47 K. Chaudhary, K. Bhakuni, N. K. Mogha, P. Venkatesu and D. T. Masram, *ACS Biomater. Sci. Eng.*, 2020, 4881–4892.